Author Manuscript

Author Manuscript

Author Manuscript

Author Manuscript

HHS Public Access

Author manuscript

J Immunol. Author manuscript; available in PMC 2018 June 01.

Published in final edited form as:

J Immunol. 2017 June 01; 198(11): 4244–4254. doi:10.4049/jimmunol.1601912.

Protein Kinase CK2 Controls the Fate Between Th17 Cell and Regulatory T Cell Differentiation CK2 Regulates the Th17/Treg Axis

Sara A Gibson[*], **Wei Yang**[*], **Zhaoqi Yan**[*], **Yudong Liu**[*], **Amber L Rowse**[*], **Amy S. Weinmann**[†], **Hongwei Qin**[*], and **Etty N. Benveniste**[*]

[*]University of Alabama at Birmingham, Department of Cell, Developmental and Integrative Biology, Birmingham, AL

[†]University of Alabama at Birmingham, Department of Microbiology, Birmingham, AL

Abstract

CK2 is a highly conserved and pleiotropic serine/threonine kinase that promotes many pro-survival and pro-inflammatory signaling pathways including PI3K/Akt/mTOR and JAK/STAT. These pathways are essential for $CD4^+$ T cell activation and polarization, but little is known about how CK2 functions in T cells. Here we demonstrate that CK2 expression and kinase activity are induced upon $CD4^+$ T cell activation. Targeting the catalytic activity of CK2 using the next generation small molecule inhibitor CX-4945 *in vitro* significantly and specifically inhibited mouse and human Th17 cell differentiation while promoting the generation of $Foxp3^+$ Tregs. These findings were associated with suppression of PI3K/Akt/mTOR activation and STAT3 phosphorylation upon CX-4945 treatment. Furthermore, we demonstrate that CX-4945 treatment inhibits the maturation of Th17 cells into inflammatory IFN-γ co-producing effector cells. The Th17/Treg cell axis and maturation of Th17 cells are major contributing factors to the pathogenesis of many autoimmune disorders, including multiple sclerosis (MS). Using a murine model of MS, experimental autoimmune encephalomyelitis (EAE), we demonstrate that *in vivo* administration of CX-4945 targets Akt/mTOR signaling in $CD4^+$ T cells and the Th17/Treg axis throughout disease. Importantly, CX-4945 treatment after disease initiation significantly reduced disease severity, which was associated with a significant decrease in the frequency of pathogenic IFN-γ^+ and GM-CSF^+ Th17 cells present in the CNS. Our data implicate CK2 as a regulator of the Th17/Treg cell axis and Th17 cell maturation, and suggest that CK2 could be targeted for the treatment of Th17 cell-driven autoimmune disorders.

INTRODUCTION

Protein kinase CK2 is a ubiquitously expressed and constitutively active serine/threonine kinase (1). It is unique in its ability to regulate numerous canonical signaling pathways

Correspondence Address: Hongwei Qin, PhD., University of Alabama at Birmingham, 1918 University Boulevard, MCLM 313, Birmingham, AL 35294. Etty N. Benveniste, Ph.D., University of Alabama at Birmingham, 510 20th Street South, FOT 1220, Birmingham, AL 35294.

Co-Corresponding Authors: Hongwei Qin, PhD., Phone: (205) 934-7668, Fax: (205) 975-5648, hqin@uab.edu. Etty N. Benveniste, Ph.D., Phone: (205) 934-7667, Fax: (205) 934-0333, tika@uab.edu

Author Manuscript Author Manuscript Author Manuscript Author Manuscript

through phosphorylation of over 500 target proteins, and is therefore capable of modulating numerous cellular processes including cell survival, proliferation and inflammation (2). Structurally, the holoenzyme is a tetramer comprised of two catalytic subunits, CK2α and/or CK2α′, associated with two regulatory subunits, CK2β. The regulatory subunit is not essential for activity, but confers specificity and therefore can affect the ability of the catalytic subunits to phosphorylate certain substrates. As such, CK2α/α′ can maintain catalytic activity in the absence of their association with CK2β, adding to the complexity of CK2 biology (3). Aberrant CK2 activity is present in a number of tumors, promoting anti-apoptotic and pro-angiogenic mechanisms that favor tumor survival and growth, and is therefore a promising target for cancer therapy (4–6). CX-4945, an ATP-competitive small molecule inhibitor of both catalytic subunits of CK2, is one of the most specific inhibitors of CK2 available and is currently in Phase 1 and 2 clinical trials for both solid and liquid tumors (6–8).

Auto-reactive $CD4^+$ T cells drive a number of autoimmune diseases including multiple sclerosis (MS), a demyelinating inflammatory disease of the CNS, and the widely used animal model of MS, experimental autoimmune encephalomyelitis (EAE) (9, 10). Once activated, complex networks of signaling pathways and transcription factors contribute to the differentiation of $CD4^+$ T cells into effector or regulatory phenotypes depending on the inflammatory environment (11, 12). In particular, PI3K/Akt/mTOR signaling is known to promote the differentiation of pro-inflammatory IFN-γ-producing Th1 cells and IL-17-producing Th17 cells, while inhibiting anti-inflammatory $Foxp3^+$ Tregs (13, 14). In addition, activation of the JAK/STAT pathway by different cytokines is essential for the production of effector molecules associated with different phenotypes. IL-12-mediated STAT4 activation and IL-6-mediated STAT3 activation are required for the Th1 and Th17 phenotypes, respectively, while sustained IL-2-mediated STAT5 activation promotes Tregs (11). Importantly, Th17 cells exhibit unique plasticity. In the presence of cytokines such as IL-23 and IL-12, Th17 cells may become ‘Th1-like’ and co-produce IFN-γ. These mature Th17 cells have been shown to be critical effector cells in MS (15, 16). In addition, both Th17 cells and Tregs require TGFβ, allowing for a degree of plasticity between the two phenotypes, which is further regulated by the balance of activated STAT3 and STAT5 (17, 18).

Although CK2 is known to promote the activity of the PI3K/Akt/mTOR and JAK/STAT pathways (19–21), little is known as to how CK2 functions in $CD4^+$ T cells. We demonstrate that CK2 protein and kinase activity are enhanced upon $CD4^+$ T cell activation. Furthermore, CK2 activity selectively promotes Th17 cell differentiation while suppressing Treg cell differentiation through modulation of mTOR and STAT3 signaling. In addition, CK2 promotes the maturation of Th17 cells into IFN-γ co-producing effectors. Importantly, inhibition of CK2 utilizing CX-4945 suppressed Th17 cell responses, promoted Tregs and was ultimately protective in EAE. Our results support that pharmacological inhibition of CK2 may be therapeutic in T cell-driven autoimmune diseases through targeting of the Th17/Treg cell axis and Th17 cell maturation.

Author Manuscript Author Manuscript Author Manuscript Author Manuscript

MATERIALS AND METHODS

Mice

C57BL/6 mice, Rag1$^{-/-}$ mice, TCR-transgenic 2D2 mice and transgenic CD45.1 mice were bred in the animal facility at the UAB. *Il17f*$^{Thy1.1}$.*Foxp3*^{GFP} reporter mice were generated in the laboratory of Dr. Casey Weaver, UAB (16, 22) and bred in the animal facility at UAB. 8–12 week old male and female mice were used for all experiments. All experiments using animals were reviewed and approved by the Institutional Animal Care and Use Committee of UAB.

Inhibitors

The CX-4945 compound was provided by Cylene Pharmaceuticals (San Diego, CA). The compound was dissolved in DMSO for *in vitro* experiments. The compound was reconstituted in sodium phosphate (25 mM) and administered via oral gavage *in vivo*. Rapamycin was purchased from Sigma Aldrich and diluted in DMSO.

Cytokines, Antibodies and Dyes

Mouse and human cytokines used for *in vitro* polarizations as well as anti-human CD3 and anti-human CD28 were purchased from Biolegend. Anti-mouse CD3, anti-mouse CD28 and mouse and human neutralizing antibodies to IL-4 and IFN-γ were purchased from BioXCell. Anti-CK2α and anti-CK2β antibodies for detection by flow cytometry were purchased from AbCam and Calbiochem, respectively. Secondary antibodies for flow cytometry were purchased from Jackson ImmunoResearch. Flow cytometry antibodies against mouse CD4, IL-17A, IFN-γ, CD25 and CD45.1 and human CD3, CD4 and Foxp3 were purchased from Biolegend. Flow cytometry antibodies against mouse CD44, Foxp3 and GM-CSF and human IL-17A were purchased from eBioscience. Aqua Live/Dead Viability dye, CFSE proliferation dye and 2-NBDG were purchased from ThermoFisher Scientific. Flow cytometry antibodies and isotype controls for phosphorylated S6, Akt, STAT3, STAT5 and SMAD2/3 were purchased from Cell Signaling. Immunoblotting antibodies against phosphorylated T389, S371 and total S6 Kinase p70 and phosphorylated S129, S473 and total Akt were purchased from Cell Signaling, and antibody against mouse β-actin was purchased from abcam.

Naïve CD4$^+$ T cell Enrichment, Activation and Polarization

Naive CD4$^+$ T cells were enriched from the spleens of 8–12 week of mice using the Naïve CD4$^+$ T cell Kit purchased from Stem Cell Technologies. Cells were cultured at a density of 0.75 – 1 x 10^6 cells/ml in RPMI supplemented with 10% FBS, L-glutamine, Hepes buffer, sodium pyruvate, β-mercaptoethanol and penicillin/streptomycin (R10). Cells were activated with plate-bound anti-CD3 (10 μg/ml) and soluble anti-CD28 (1 μg/ml) for activation and polarization experiments. Th1 polarizing conditions were IL-12 (10 ng/ml) and anti-IL-4 (10 μg/ml); Th17 conditions were IL-6 (20 ng/ml), TGFβ1 (2.5 ng/ml), IL-23 (10 ng/ml), anti-IL-4 (10 μg/ml), and anti-IFN-γ (10 μg/ml); and Treg polarizing conditions were TGFβ1 (5 ng/ml), IL-2 (5 ng/ml), anti-IL-4 (10 μg/ml), and anti-IFN-γ (10 μg/ml). Polarizations were ended at 72 h unless otherwise noted. For cytokine signaling experiments, cells were

Author Manuscript Author Manuscript Author Manuscript Author Manuscript

activated overnight, resuspended in serum free media +/− CX-4945 for 4 h, and then stimulated with IL-6 (10 ng/ml) for 2 h or IL-2 (5 ng/ml) or TGFβ1 (5 ng/ml) for 30 min.

RNA Interference

siRNA transfection was performed using the Amaxa Mouse T Cell Nucleofector Kit, purchased from Lonza, as previously described (23). Non-targeting and CK2α-targeting siRNA constructs were purchased from Dharmacon. Transfection efficiency, as measured by eGFP transfection, was 20–30%.

Flow Cytometry

For surface protein detection, cells were incubated with Fc Block (2.4G2) for 15 min, washed and incubated with viability dye and anti-surface protein antibodies. For intracellular CK2 subunit and phosphorylated protein detection cells were permeabilized with 70% and 90% MeOH, respectively. For cytokine detection, cells were stimulated with PMA (25 ng/ml) and Ionomycin (1 μg/ml) in the presence of GolgiStop (BD Biosciences) for 4 h and permeabilized using the Foxp3 Staining Buffer Kit (eBioscience). For glucose uptake, cells were incubated with 2-NBDG (5 nM) for 30 min at 37°C, washed and stained for viability and surface markers (24). Stained cells were run on an LSRII flow cytometer (BD Biosciences), and data was analyzed using FlowJo Software (TreeStar). Representative flow plots are gated on live, $CD4^+$ cells, unless otherwise noted.

Immunoblotting

$CD4^+$ T cells were lysed in buffer containing 1% Triton X-100 (Sigma-Aldrich), and protein lysate was separated by electrophoresis, transferred to a nitrocellulose membrane and blotted with immunoblotting antibodies, as previously described (25).

CK2 Kinase Activity

The Casein Kinase 2 Assay Kit (Millipore) was used to assess CK2 kinase activity. Cells were lysed and both catalytic subunits, CK2α and CK2α′, were immunoprecipitated. Resulting lysates were assayed for CK2 kinase activity (21).

Proliferation and Suppression Assays

For *in vitro* proliferation assays, naïve $CD4^+$ T cells were incubated in CFSE dye, washed and activated with plate-bound anti-CD3 and soluble CD28 antibodies. At 72 h, CFSE dilution was determined by flow cytometry. For suppression assays, naïve $CD4^+$ T cells from $Il17f^{Thy1.1}.Foxp3^{GFP}$ mice were polarized in indicated conditions for 72 h. GFP^+ cells were sorted using a FACS Aria (BD Biosciences) and co-cultured at a 1:4 ratio with CFSE-labeled $CD45.1^+$ naïve $CD4^+$ T cells activated with plate-bound anti-CD3 and soluble CD28 antibodies. At 72 h, CFSE dilution of $CD45.1^+$ cells was determined by flow cytometry.

Human T Cell Polarizations

Human blood was obtained with the appropriate approval from the UAB Institutional Review Board for Human Use. PBMCs were isolated from human blood and plated at a density of 1×10^6 cells/ml in R10 media. Cells were activated with plate-bound anti-CD3

Author Manuscript Author Manuscript Author Manuscript Author Manuscript

(10 μg/ml) and soluble anti-CD28 (1 μg/ml). Th17 cells were polarized in the presence of IL-1β (10 ng/ml), IL-6 (10 ng/ml), IL-23 (10 ng/ml), TGFβ1 (2.5 ng/ml) and neutralizing antibodies to IL-4 (10 μg/ml) and IFN-γ (10 μg/ml). After 6 days, polarization was assessed by flow cytometry.

Plasticity Assay

To model Th17 cell plasticity *in vitro* a protocol was adapted from the literature (26). Naïve $CD4^+$ T cells from *Il17f*$^{Thy1.1}$.*Foxp3*^{GFP} mice were cultured in Th17 conditions. At 72 h, $Thy1.1^+$ cells were sorted and restimulated with plate-bound anti-CD3, soluble anti-CD28 and either IL-12 (10 ng/ml), or IL-2 (5 ng/ml) and TGFβ1 (5 ng/ml) +/− CX-4945 for an additional 48 h, then assayed for IFN-γ or Foxp3 expression, respectively.

RNA Isolation, RNA-Sequencing and qRT-PCR

Total RNA was isolated from cells using Trizol extraction. Quality was checked by nanodrop, and 5 μg was submitted to GeneWiz (South Plainfield, NJ) for RNA-sequencing and bioinformatic analysis. RNA-seq data will be publicly available at time of publication, accession number: GSE86976. Access link: https://www.ncbi.nlm.nih.gov/geo/query/acc.cgi?token=qvedemwuzfmznah&acc=GSE86976 Further pathway analysis was performed using the Gene Set Enrichment Analysis available through the Broad Institute. For quantitative RT-PCR analysis, 500 to 1000 ng of RNA was used to reverse transcribe into cDNA. cDNA was subjected to qRT-PCR using TaqMan primers purchased from ThermoFisher Scientific. The data were analyzed using the comparative cycle threshold method to obtain relative quantitation values.

EAE Induction, Assessment and Cell Isolation

For adoptive transfer EAE, a protocol was adapted from the literature (27). Naïve $CD4^+$ T cells from 2D2 mice, with TCRs specific to $MOG_{35–55}$ (28), were activated with anti-CD3 and anti-CD28 and polarized to the Th17 phenotype for 72 h, restimulated with anti-CD3 and anti-CD28 antibodies overnight and 2 x 10^6 cells were transferred to $Rag1^{-/-}$ mice via intraperitoneal injection. Active EAE was induced in C57BL/6 mice using $MOG_{35–55}$ emulsified in complete Freund's adjuvant purchased from Hooke Laboratories, as previously described (25). Mice were monitored daily and scored on a scale of 0 to 5: 0, no disease; 1, tail paralysis; 2, hind limb paresis; 3, complete hind limb paralysis; 4, front limb weakness and hind limb paralysis; and 5, moribund state. Total $CD4^+$ T cells were enriched from the spleens of immunized mice using the CD4 T cell isolation kit (Milteny). Mononuclear cells were isolated from the spinal cords of immunized mice using a Percoll gradient, as previously described (25, 29), and assessed by flow cytometry.

Statistics

Levels of significance for comparison between two groups were determined by one-sided two-sample Mann–Whitney rank sum test, in the case of EAE scores, and the Student *t* test distribution. A p value <0.05 was considered statistically significant. All error bars represent SEM.

Author Manuscript Author Manuscript Author Manuscript Author Manuscript

RESULTS

CK2 Subunit Protein Expression and Kinase Activity are Induced Upon CD4+ T Cell Activation

We first determined the expression pattern of CK2α, the major catalytic subunit of CK2, and CK2β, the regulatory subunit of CK2, in naïve and activated primary murine $CD4^+$ T cells. Expression of both CK2α and CK2β substantially increased upon activation with anti-CD3 and anti-CD28 antibodies in a time-dependent manner (Figure 1A). Increases in protein expression also correlated with a significant increase in CK2α and CK2β mRNA compared to naïve cells by 72 h (Figure 1B), suggesting the induction occurs at least partially at the transcriptional level. In addition to subunit expression, a number of factors can contribute to overall CK2 kinase activity (1). Importantly, induction of CK2 expression upon activation was associated with a significant increase in overall kinase activity (Figure 1C). These results demonstrate an induction of CK2 expression and activity upon $CD4^+$ T cell activation and suggest a potential role for CK2 in $CD4^+$ T cell function.

CK2 Kinase Activity Promotes Akt/mTOR Signaling in CD4+ T Cells but is Not Required for CD4+ T Cell Activation or Proliferation

CK2 regulates a number of pathways important for $CD4^+$ T cell activation and differentiation including the PI3K/Akt/mTOR pathway (19, 20). We stimulated naïve $CD4^+$ T cells with anti-CD3 and anti-CD28 antibodies in the absence or presence of the CK2 inhibitor CX-4945 (2 μM) or rapamycin (100 nM) for 24 h, when CK2 is robustly induced, and then examined mTOR activation. The CX-4945 dose was chosen after determining the dose-dependent effect of CX-4945 treatment on cell viability. Two μM CX-4945 was the maximum dose tested that had no effect on viability of the cells (Supplemental Figure 1). CX-4945 treatment resulted in partial inhibition of mTOR activity as indicated by a decrease in phosphorylation of the downstream target of mTORC1, S325/236 S6 kinase p70, and the downstream target of mTORC2, S473 Akt (Figure 1D). The partial inhibition of mTORC1 signaling by CX-4945 was less than the near complete inhibition caused by rapamycin, while inhibition of mTORC2 signaling was comparable between the two inhibitors (Figures 1D, 1E and 1F). Considering that rapamycin is a direct inhibitor of mTORC1 while inhibition of mTORC2 is indirect (30), we conclude that CX-4945 acts to promote signaling through both complexes, but is not necessarily required for their activation. Studies have demonstrated that inhibition of mTOR activity by rapamycin treatment or genetic deletion has little effect on the expression of T cell activation markers such as CD25 and CD69, but greatly inhibits $CD4^+$ T cell proliferation (13, 31). To determine if CK2 is critical for activation in response to TCR and costimulatory signals, naïve $CD4^+$ T cells were activated with anti-CD3 and anti-CD28 antibodies for 24 h in the absence or presence of CX-4945 or rapamycin. CX-4945 treatment did not have a substantial impact on expression of the activation markers CD25 and CD69 after 24 h, compared to minimal inhibition by rapamycin (Figures 1G and 1H). CX-4945 treatment, however, did result in a small, but significant, decrease in IL-2 production after 24 h (Figure 1I). To determine if CX-4945 treatment had any effect on autocrine IL-2 signaling in culture, cells were stained for phosphorylated STAT5 Y694. Although IL-2 levels were reduced, STAT5 signaling in response to autocrine IL-2 was intact in the presence of CX-4945 (Figure 1J). To assess

Author Manuscript Author Manuscript Author Manuscript Author Manuscript

effects on proliferation, naïve $CD4^+$ T cells were incubated in CFSE dye, and activated in the absence or presence of CX-4945 or rapamycin for 72 h. Inhibition of CK2 with CX-4945 had no significant effect on the ability of $CD4^+$ T cells to proliferate, in contrast to substantial inhibition with rapamycin (Figures 1K and 1L). Together, these data demonstrate that although CK2 promotes mTOR signaling, its activity is not required for $CD4^+$ T cell activation or proliferation.

CK2 Inhibition Selectively Suppresses Th17 Cell Differentiation and Promotes the Generation of Tregs *In Vitro*

Although the inhibition of Akt/mTOR with CX-4945 compound is partial, the signal strength and duration through the Akt/mTOR pathway in response to TCR and costimulation have been shown to be critical regulators of $CD4^+$ T cell differentiation. Strong signals promote the inflammatory effector phenotypes, while weaker signals can bias the cell to become a Treg (32, 33). To begin investigating the potential role for CK2 in regulating $CD4^+$ T cell differentiation, naïve $CD4^+$ T cells were polarized to the Th1, Th17 and Treg phenotypes in the absence or presence of CX-4945. Interestingly, CX-4945 treatment had no effect on the frequency of IFN-γ^+ cells in Th1 polarizing conditions (Figure 2A). CX-4945 treatment, however, did result in a significant decrease in the frequency of IL-$17A^+$ cells in Th17 polarizing conditions (Figures 2B, 2D and 2E). This finding is consistent with the previously defined role of CK2 in transducing signals through CD5 to promote Th17 cell differentiation, but not Th1, described by the Raman group (34, 35). Alternatively, CX-4945 treatment significantly enhanced the generation of $Foxp3^+$ cells in Treg conditions (Figure 2C). These results demonstrate that CK2 functions in $CD4^+$ T cells to promote Th17 cell differentiation while inhibiting the generation of Tregs.

CK2 Regulates the Th17/Treg Cell Axis Through Modulation of Cytokine Signaling

Mechanistically, overlapping programs allow for a degree of plasticity between the Th17 and Treg phenotypes (36, 37). CX-4945 treatment not only significantly suppressed the generation of IL-$17A^+$ Th17 cells, but also reciprocally promoted the generation of $Foxp3^+$ cells under Th17 conditions (Figures 2D and 2E), implicating CK2 as a key regulator of the Th17/Treg cell axis.

Furthermore, CX-4945 treatment did not result in increased Foxp3 expression in the absence of cytokines (Th0) or Th1 polarizing conditions (Supplemental Figure 2A). This finding suggests that effect of CK2 inhibition on Akt/mTOR signaling is not sufficient to promote the generation of Tregs. In addition to the PI3K/Akt/mTOR pathway, the balance of IL-6-induced phosphorylated STAT3 and IL-2-induced phosphorylated STAT5 are important regulators of the Th17/Treg axis (17, 18). We have previously shown that CK2 can directly promote the activation of STAT proteins through phosphorylation of upstream Janus Kinases (21). To determine the potential influence of CK2 activity on phosphorylation of STAT3 and STAT5, naïve $CD4^+$ T cells were activated overnight, resuspended in serum-free media in the absence or presence of CX-4945 for 4 h, and then stimulated with IL-6 or IL-2 for 2 h or 30 min, respectively. CX-4945 treatment significantly inhibited the phosphorylation of STAT3 Y705 and in response to IL-6 (Figure 2F). Alternatively, CX-4945 did not inhibit IL-2-induced phosphorylation of STAT5 Y694 (Figure 2G). Both Th17 and Treg cell

Author Manuscript Author Manuscript Author Manuscript Author Manuscript

differentiation require TGFβ1, which primarily signals through Smad proteins (37). CX-4945 treatment had no significant effect on TGFβ1-induced phosphorylation of S465/467 Smad2 and S423/425 Smad3 (Figure 2H). Together, these data indicate the CK2 promotes Th17 cell differentiation through enhancing the phosphorylation of STAT3. Therefore, inhibition of CK2 results in decreased STAT3 activation and allows signals through STAT5 and SMAD2/3 to promote Foxp3 expression.

We next sought to determine if the Foxp3$^+$ cells generated in Th17 conditions were functionally suppressive. We utilized IL-17F and Foxp3 double reporter mice, in which IL-17F expression is reported by surface Thy1.1 expression, and Foxp3 is reported by GFP (16, 22). Naïve CD4$^+$ T cells from *Il17f*$^{Thy1.1}$.*Foxp3*^{GFP} mice were cultured under Th17 conditions in the presence of CX-4945 or under Treg conditions, and GFP$^+$ cells were sorted and co-cultured with CFSE-labeled naïve effector cells stimulated with anti-CD3 and anti-CD28 antibodies. Foxp3$^+$ cells generated under Th17 conditions in the presence of CX-4945 (Th17+CX) were able to suppress effector cell proliferation equivalent to Foxp3$^+$ cells generated under Treg conditions (Figure 2I). Therefore, CK2 promotes Th17 cell differentiation while actively suppressing the generation of functional Foxp3$^+$ Tregs under Th17 conditions, further implicating CK2 as a critical regulator of the Th17/Treg axis.

Genetic Targeting of CK2α Targets the Th17/Treg Axis

Although CX-4945 is one of the most selective CK2 inhibitors available, off-target effects have been described (38). As such, we next sought to validate the regulation of the Th17/Treg axis by CK2 utilizing a genetic approach. Since deletion of the major catalytic subunit of CK2, CK2α, is embryonic lethal (39), we utilized siRNA to knock-down CK2α. CD4$^+$ T cells were transfected with either non-targeting siRNA or siRNA targeted to CK2α, and cultured under Th17 conditions. Importantly, targeting of CK2α with siRNA inhibited Th17 cell differentiation and reciprocally promoted the generation of Foxp3$^+$ Tregs (Figures 2J and 2K).

CK2 Inhibition Targets the Human Th17/Treg Axis

To determine if CK2 regulates the human Th17/Treg axis *in vitro*, and could therefore potentially regulate the Th17/Treg cell axis during human disease, PBMCs were enriched from human blood and polarized for 6 days under Th17 conditions in the absence or presence of CX-4945. CX-4945 treatment resulted in a significant decrease in the frequency of IL-17A$^+$ cells and a significant increase in the frequency of Foxp3$^+$ cells under Th17 conditions (Figures 2L and 2M). These data demonstrate that CK2 promotes the differentiation of human Th17 cells while reciprocally suppressing the generation of Foxp3$^+$ Tregs, similar to murine CD4$^+$ T cells.

CK2 Inhibition Results in Decreased Th17-associated Effector and Metabolic Gene Expression

To comprehensively investigate changes to the Th17 program in response to CK2 inhibition, we performed RNA-sequencing (RNA-seq) analysis on cells cultured in Th17 conditions for 72 h in the absence or presence of CX-4945. Over 1500 genes had a 2-fold or greater change in expression as a result of CX-4945 treatment (Figure 3A). We performed an unbiased

Author Manuscript Author Manuscript Author Manuscript Author Manuscript

Gene Set Enrichment Analysis to determine the major Th17-associated pathways affected by CX-4945 treatment. We limited this analysis to a set of 134 genes that were the most highly expressed in untreated cells and were inhibited at least two-fold by CX-4945 treatment. The pathway analysis revealed a significant overlap between genes that were inhibited by CX-4945 treatment and genes that are induced in Th17 polarizing conditions as well as genes associated with both hypoxia and glycolysis (Figure 3B). These data indicate that CK2 broadly influences the expression of many genes involved in programming the Th17 phenotype, including transcription factors, effector genes, and genes that regulate the metabolic state of the cell. Interestingly, genes that were decreased in the presence of CX-4945 were particularly enriched for genes associated with pathogenic Th17 cells grown in pathogenic conditions, including additional polarizing cytokines such as TGFβ3 and IL-1. Along with IL-23, these cytokines have been shown to program more pathogenic effector Th17 cells in the context of autoimmunity compared to IL-6 and TGFβ1 alone (40).

We next performed a targeted analysis of Th17 effector genes. CX-4945 treatment significantly inhibited the expression of genes for transcription factors essential for Th17 differentiation including *Rorc, Rora, Ahr* and *Hif1a* (Figure 3C). Consistent with a broad change in Th17-programming capacity, there was a global decrease in Th17-associated effector genes such as *Il17a, Il17f, Ccr6* and *Il23r* (Figure 3C). Alternatively, and consistent with our findings at the protein level (Figures 2D and 2E), the Treg associated transcription factor *Foxp3* was significantly increased (Figure 3C). Importantly, the effect of CX-4945 on transcription of a panel of Th17 effector genes along with *Foxp3* was validated by qPCR (Figure 3D).

Recent studies have highlighted the importance of metabolism in the induction of $CD4^+$ T cell phenotypes (41, 42). In particular, Th17 cells are characterized by a preferential use of glycolysis and expression of hypoxia-inducible genes while Treg cells are characterized by the use of mitochondrial, oxidative metabolism. (43, 44). Further analysis of the RNA-seq data revealed a global decrease in genes associated with glycolysis and hypoxia and a reciprocal increase in genes associated with mitochondrial metabolism in CX-4945 treated cells compared to untreated cells (Figures 3E). A panel of these metabolic genes were validated by qPCR (Figure 3F). To determine if the change in gene expression observed with CX-4945 treatment correlated with changes in glycolytic activity of cells, we performed a 2-NBDG uptake assay. CX-4945 resulted in a significant decrease in the uptake of the fluorescent glucose analog (Figure 3G), providing evidence that CX-4945 treatment results in a significant decrease in glycolytic activity.

CK2 Inhibition Suppresses IL-12-induced IFN-γ Production By Th17 Cells

IL-17-producing Th17 cells can gain the ability to co-produce additional inflammatory cytokines such as IFN-γ *in vivo* in response to cytokines such as IL-12 and IL-23. These mature, pathogenic Th17 cells are critical for neuroinflammation during EAE (15, 16). To determine if CK2 kinase activity contributes to the maturation of Th17 cells into $IL\text{-}17A^+IFN\text{-}\gamma^+$ cells, naïve $CD4^+$ T cells from *Il17f*$^{Thy1.1}$.*Foxp3*^{GFP} reporter mice were cultured in Th17 conditions. After 72 h of polarization, $Thy1.1^+GFP^-$ cells were sorted and restimulated with anti-CD3 and anti-CD28 antibodies in the presence of IL-12 and in the

Author Manuscript Author Manuscript Author Manuscript Author Manuscript

absence or presence of CX-4945. After 48 h of restimulation, CX-4945 treatment significantly decreased the production of IFN-γ from Th17 cells in response to IL-12 (Figures 4A and 4B). In these conditions, or upon addition of TGFβ1 and IL-2 during restimulation, CX-4945 treatment did not cause an increase in Foxp3 expression in Th17 cells (Supplemental Figure 2B). These results suggest that CK2 is not required to suppress Foxp3 expression after cells have committed to the Th17 lineage. In addition, induction of Foxp3 expression can not explain the inhibition of IFN-γ production from Th17 cells. Studies have demonstrated that the production of IFN-γ by Th17 cells is mediated by transcription factors including T-bet and Runx3 (26). The expression of *Ifng*, *Tbx21* and *Runx3* were significantly decreased in Th17 cells restimulated in the presence of CX-4945 as compared to untreated cells (Figure 4C). These data demonstrate that CK2 activity promotes IFN-γ production by Th17 cells and the expression of transcription factors necessary for maturation into pathogenic Th17 effector cells.

CK2 Promotes the Pathogenicity of Th17 Cells in Adoptive Transfer Experimental Autoimmune Encephalomyelitis

To determine how CK2 activity contributes to the differentiation of $CD4^+$ T cells into Th17 cells capable of functioning as pathogenic effector cells *in vivo*, we utilized Th17-mediated adoptive transfer EAE with $CD4^+$ T cells isolated from 2D2 mice (27). $CD4^+$ T cells were enriched from 2D2 mice, polarized under Th17 conditions for 72 h, and then restimulated with anti-CD3 and anti-CD28 antibodies for an additional 24 h. DMSO (Vehicle) or CX-4945 was added to the cells either at the initial polarization only (day 0) or during restimulation only (day 3). On day 4, 2 x 10^6 cells were transferred via intraperitoneal injection into $Rag1^{-/-}$ mice, and recipients were monitored daily for signs of classical EAE (Figure 4D). Mice receiving cells either polarized under Th17 conditions in the presence of CX-4945 (day 0), or restimulated after initial polarization in the presence of CX-4945 (day 3), experienced a significantly delayed progression of EAE disease (Figure 4E). These results indicate that CK2 activity promotes the pathogenic effector function of Th17 cells. Mice in both CX-4945 treatment groups can reach the same peak score by day 30 post transfer (data not shown). At disease peak, CX-4945 treated cells reach similar frequencies of IL-$17A^+$ and IL-$17A^+$IFN-γ^+ cells to control cells in the spinal cords of recipient mice, suggesting recovery in the absence of CX-4945 (data not shown).

CK2 Expression is Enhanced in $CD4^+$ T Cells in the Context of EAE

To determine the expression and function of CK2 in $CD4^+$ T cells activated during an *in vivo* inflammatory autoimmune response, active EAE was induced in C57BL/6 mice by immunization with $MOG_{35–55}$ peptide emulsified in CFA (Figure 5A). We first examined the expression of CK2α protein in $CD4^+$ T cells at two timepoints during EAE disease development; pre-onset (day 9) and progression (day 12) (Figure 5A). At day 9, $CD4^+$ T cells from the draining lymph nodes expressed elevated CK2α protein compared to $CD4^+$ T cells from an unimmunized control mouse (Figure 5A). On day 12, $CD4^+$ T cells from the spinal cord expressed higher levels of CK2α compared to $CD4^+$ T cells from an unimmunized control mouse (Figure 5A).

Author Manuscript Author Manuscript Author Manuscript Author Manuscript

CX-4945 Pre-treatment Reduces EAE Disease Severity

For functional *in vivo* studies, mice were administered the CX-4945 compound orally at 20 mg/kg daily. This dose was determined to be well tolerated by the C57BL/6 strain, as CX-4945 treatment did not result in accelerated weight loss compared to vehicle-treated controls (Supplemental Figure 3). To determine the effect of CK2 inhibition on EAE disease course, mice were treated daily beginning one week before immunization and monitored for clinical symptoms. CX-4945 treatment significantly reduced disease severity (Figure 5B). To determine if CK2 inhibition targeted the PI3K/Akt/mTOR pathway *in vivo*, $CD4^+$ cells were enriched from the spleens at day 9-post immunization (PI), lysed and immunoblotted for downstream targets of the Akt/mTOR pathway. CX-4945 treatment led to substantial decreases in phosphorylation of S129 Akt, a CK2 specific phosphorylation site, S473 Akt, and T389 S6 Kinase p70 (Figure 5C), demonstrating that CK2 contributes to the activation of the Akt/mTOR pathway in $CD4^+$ T cells during EAE.

In order to determine the consequence of CX-4945 pre-treatment on the phenotype of $CD4^+$ T cells present in the CNS, mononuclear cells were enriched from the spinal cords of Vehicle- and CX-4945-treated mice at day 23 PI. FACS analysis revealed a significant increase in the frequency of $CD25^+Foxp3^+$ Tregs in the treated group (Figure 5D). These data demonstrate that protection conferred by CX-4945 treatment is associated with a decrease in Akt/mTOR signaling, resulting in an increase in the generation of Tregs during disease resolution.

Inhibition of CK2 Targets the Th17/Treg Axis During the Initiation of EAE

To determine if CK2 inhibition during disease initiation is sufficient to target $CD4^+$ T cell differentiation during EAE, mice were treated with CX-4945 from days 0 to 7 PI. At day 7, before the onset of clinical symptoms, $CD4^+$ T cells from the draining lymph nodes were assessed for IFN-γ and IL-17A expression. Consistent with our *in vitro* data (Figures 2A and 2B), CX-4945 treatment caused a significant decrease in the frequency of $IL\text{-}17A^+CD4^+CD44^+$ T cells in the draining lymph nodes (dLN), with no effect on IFN-$\gamma^+CD4^+CD44^+$ T cells (Figure 5E). In addition, treatment resulted in a significant increase in the frequency of Tregs present in the spleen (Figure 5F), demonstrating that inhibition of CK2 targets the Th17/Treg axis in the periphery during the initiation phase of EAE.

Therapeutic CX-4945 Treatment Reduces EAE Disease Severity

To test the therapeutic efficacy of CX-4945 in active EAE, mice were immunized on day 0, and treated with CX-4945 or vehicle for one week starting at the onset of clinical symptoms. Therapeutic CX-4945 treatment significantly reduced the severity of clinical symptoms throughout the remaining course of disease (Figure 6A).

Unlike CX-4945 pre-treatment, protection observed with the therapeutic treatment could not be explained by promotion of Tregs, as no difference was observed in Treg frequencies during disease resolution (Figure 6B). Therefore, to determine the effect of CX-4945 treatment after disease initiation on effector $CD4^+$ T cells present in the CNS, mice were immunized on day 0 and treated with CX-4945 from days 7 to 14 PI, when mice are experiencing clinical disease progression. CX-4945 treatment resulted in significantly

Author Manuscript Author Manuscript Author Manuscript Author Manuscript

decreased frequencies of IL-17A$^+$ effector T cells present in the spinal cord, with no significant effect on the frequencies of IL-17A$^-$IFN-γ^+ cells (Figure 6C). Importantly, treatment after disease initiation resulted in a significant decrease in the frequency of IL-17A$^+$IFN-γ^+ pathogenic effector cells present in the spinal cord (Figure 6C). In addition to IFN-γ, Th17 cells are a major source of local GM-CSF production in the CNS during EAE. Furthermore, Th17 cell-derived GM-CSF is critical for disease progression (45, 46). While CX-4945 treatment had no significant effect of the frequency of IL-17A$^-$GM-CSF$^+$ cells in the spinal cord, treatment did result in a significant decrease in the frequency of IL-17A$^+$ GM-CSF$^+$ cells (Figure 6D). These data demonstrate that CX-4945 treatment is capable of suppressing the generation of the pathogenic IFN-γ- and GM-CSF-producing Th17 cells, ultimately leading to protection during active EAE.

DISCUSSION

CK2 is involved in a vast number of biological processes, with more that 2,000 putative phosphorylation sites in the human proteome (6). Our findings document an important role for CK2 in adaptive immunity as a critical regulator of the Th17/Treg cell axis. Inhibition of CK2 restrains the formation of both murine and human Th17 cells and promotes the development of anti-inflammatory Foxp3$^+$ Tregs. We demonstrate that CK2 activity promotes activation of the signaling pathways essential for the Th17 phenotype, notably Akt/mTOR and STAT3, and subsequent expression of Th17-associated transcription factors and effector genes. Our findings can be explained by the ability of CK2 to enhance Akt/mTOR activation, regulate the balance of activated STAT3 to activated STAT5 and leave TGFβ1 signaling unaffected, all of which are critical for the development of Tregs (13, 17, 18). Our RNA-seq data also revealed global changes in the metabolic phenotype of the cells as a result of CK2 inhibition. Treatment with CX-4945 resulted in a shift from a Th17-associated glycolytic metabolic gene expression profile to expression of genes associated with oxidative metabolism, preferred by Tregs (41, 42). Further, a 2-NBDG uptake assay confirmed that CX-4945 treatment resulted in a significant decrease in glycolytic activity. Although a more thorough analysis of CD4$^+$ T cell metabolism is needed, these findings suggest that CK2 can direct the metabolic fate of the cell, which could play a major role in its control of CD4$^+$ T cell differentiation.

CX-4945 treatment was capable of inhibiting the Akt/mTOR pathway and targeting the Th17/Treg axis *in vivo* during EAE, and was ultimately effective in decreasing the severity of clinical symptoms. As this manuscript was in preparation, Ulges and colleagues (47) reported a protective effect of CX-4945 *in vivo* in EAE, which was also associated with an inhibition of Th17 cells and generation of Tregs. Thus our findings confirm that CK2 is critical in the control of the Th17/Treg axis during EAE.

Our studies, however, revealed several unique features regarding CK2 and CD4$^+$ T cells. We demonstrate that CK2 mRNA, protein expression and kinase activity are very low in naïve CD4$^+$ T cells, and are strongly induced upon *in vitro* activation. To our knowledge, this pattern of expression is unique to CD4$^+$ T cells and quite interesting in the context of CK2 biology. In addition, the delayed but robust induction of the transcription of CK2 mRNA is interesting, and further study may reveal novel transcriptional and post-transcriptional

Author Manuscript Author Manuscript Author Manuscript Author Manuscript

regulation of protein expression that are currently not well understood. Importantly, we demonstrate that CK2 expression in $CD4^+$ T cells is strongly induced *in vivo* under conditions that promote the autoimmune disease EAE, suggesting that auto-reactive $CD4^+$ T cells with high CK2 expression and activity may be targeted by CK2 inhibition. In addition, we describe an essential role for CK2 activity in promoting Th17 cell maturation into truly pathogenic effectors capable of co-producing the cytokine IFN-γ *in vitro.* Furthermore, the *in vivo* therapeutic efficacy of CX-4945 treatment after disease initiation was associated with a decrease in IFN-γ^+ and GM-CSF^+ Th17 cells in the CNS. This important finding demonstrates that CK2 contributes to the maintenance and maturation of cells committed to the Th17 lineage, suggesting cells may be therapeutically targeted after initial activation during disease.

Our results demonstrating that *in vivo* CX-4945 treatment inhibits phosphorylation of S129 Akt, a specific CK2 substrate, suggests that inhibition of CK2 kinase activity conferred by the catalytic subunits is associated with the inhibition of Th17 cells and promotion of Tregs. Utilizing a genetic approach, we further demonstrate that knock-down of the major catalytic subunit, CK2α, in $CD4^+$ T cells inhibits Th17 cell differentiation while promoting Tregs. Ulges and colleagues, however, demonstrated that ablation of CK2β in $CD4^+$ T cells was sufficient to target the Th17/Treg axis (47). These results collectively implicate the involvement of both subunits in regulating the differentiation and function of $CD4^+$ T cells. This is particularly interesting considering the essential role of CK2β in Tregs previously described by the same group (48). Treg specific deficiency of CK2β resulted in spontaneous development of uncontrolled Th2-mediated lung inflammation. These findings highlight the complexity of CK2 biology in regards to $CD4^+$ T cell function and the need for further study.

Ultimately, our findings characterize an essential role of CK2 in regulating $CD4^+$ T cell fate. The capacity of CK2 to direct vast gene expression changes within the cell and functional outcomes is a testament to the immense control it has over the phosphoproteome, making it a powerful therapeutic target. Furthermore, our findings demonstrate that CK2 is a critical regulator the Th17/Treg cell axis and Th17 cell maturation, which has far-reaching implications for a number of diseases in which $CD4^+$ T cells play an important role.

Supplementary Material

Refer to Web version on PubMed Central for supplementary material.

Acknowledgments

We thank Dr. Denis Drygin (Cylene Pharmaceuticals) for providing CX-4945, Dr. Casey Weaver for generously providing mice, Dr. David Crossman for RNA-sequencing advice, and Dr. Laurie Harrington, Dr. Hui Hu, Dr. Chander Raman, Boyoung Shin and Danielle Chisolm for helpful discussions. We thank Dr. Steffanie Sabbaj for her collaboration with the human work. We thank the Comprehensive Flow Cytometry Core at UAB.

This work was funded by National Institute of Health grants R01NS057563 and R01CA194414 (E.N.B.), T32AI00705 (S.A.G.), and R01AI061061 and R01AI113026 (A.S.W.). The Flow Cytometry Core at UAB is supported by NIH grants P30AR048311 and NIH P30AI27667.

Author Manuscript Author Manuscript Author Manuscript Author Manuscript

Abbreviations Used in this Article

EAE	experimental autoimmune encephalomyelitis
MS	multiple sclerosis
PI	post immunization
dLN	draining lymph node
SC	spinal cord

References

1. Litchfield DW. Protein kinase CK2: structure, regulation and role in cellular decisions of life and death. Biochem J. 2003; 369:1–15. [PubMed: 12396231]
2. Meggio F, Pinna LA. One-thousand-and-one substrates of protein kinase CK2? FASEB J. 2003; 17:349–368. [PubMed: 12631575]
3. Filhol O, Nueda A, Martel V, Gerber-Scokaert D, Benitez MJ, Souchier C, Saoudi Y, Cochet C. Live-cell fluorescence imaging reveals the dynamics of protein kinase CK2 individual subunits. Mol Cell Biol. 2003; 23:975–987. [PubMed: 12529402]
4. Duncan JS, Litchfield DW. Too much of a good thing: The role of protein kinase CK2 in tumorigenesis and prospects for therapeutic inhibition of CK2. Biochim Biophys Acta. 2008; 1784:33–47. [PubMed: 17931986]
5. Trembley JH, Chen Z, Unger G, Slaton J, Kren BT, Van Waes C, Ahmed K. Emergence of protein kinase CK2 as a key target in cancer therapy. Biofactors. 2010; 36:187–195. [PubMed: 20533398]
6. Rabalski AJ, Gyenis L, Litchfield DW. Molecular Pathways: Emergence of Protein Kinase CK2 (CSNK2) as a Potential Target to Inhibit Survival and DNA Damage Response and Repair Pathways in Cancer Cells. Clin Cancer Res. 2016; 22:2840–2847. [PubMed: 27306791]
7. Siddiqui-Jain A, Drygin D, Streiner N, Chua P, Pierre F, O'Brien SE, Bliesath J, Omori M, Huser N, Ho C, Proffitt C, Schwaebe MK, Ryckman DM, Rice WG, Anderes K. CX-4945, an orally bioavailable selective inhibitor of protein kinase CK2, inhibits prosurvival and angiogenic signaling and exhibits antitumor efficacy. Cancer Res. 2011; 70:10288–10298.
8. Chon HJ, Bae KJ, Lee Y, Kim J. The casein kinase 2 inhibitor, CX-4945, as an anti-cancer drug in treatment of human hematological malignancies. Front Pharmacol. 2015; 6:70. [PubMed: 25873900]
9. Fletcher JM, Lalor SJ, Sweeney CM, Tubridy N, Mills KH. T cells in multiple sclerosis and experimental autoimmune encephalomyelitis. Clin Exp Immunol. 2010; 162:1–11. [PubMed: 20682002]
10. Goverman J. Autoimmune T cell responses in the central nervous system. Nat Rev Immunol. 2009; 9:393–407. [PubMed: 19444307]
11. DuPage M, Bluestone JA. Harnessing the plasticity of CD4(+) T cells to treat immune-mediated disease. Nat Rev Immunol. 2016; 16:149–163. [PubMed: 26875830]
12. Kanno Y, Vahedi G, Hirahara K, Singleton K, O'Shea JJ. Transcriptional and epigenetic control of T helper cell specification: molecular mechanisms underlying commitment and plasticity. Annu Rev Immunol. 2012; 30:707–731. [PubMed: 22224760]
13. Delgoffe GM, Kole TP, Zheng Y, Zarek PE, Matthews KL, Xiao B, Worley PF, Kozma SC, Powell JD. The mTOR kinase differentially regulates effector and regulatory T cell lineage commitment. Immunity. 2009; 30:832–844. [PubMed: 19538929]
14. Delgoffe GM, Pollizzi KN, Waickman AT, Heikamp E, Meyers DJ, Horton MR, Xiao B, Worley PF, Powell JD. The kinase mTOR regulates the differentiation of helper T cells through the selective activation of signaling by mTORC1 and mTORC2. Nat Immunol. 2011; 12:295–303. [PubMed: 21358638]

Author Manuscript Author Manuscript Author Manuscript Author Manuscript

15. Kebir H, Ifergan I, Alvarez JI, Bernard M, Poirier J, Arbour N, Duquette P, Prat A. Preferential recruitment of interferon-gamma-expressing TH17 cells in multiple sclerosis. Ann Neurol. 2009; 66:390–402. [PubMed: 19810097]
16. Lee YK, Turner H, Maynard CL, Oliver JR, Chen D, Elson CO, Weaver CT. Late developmental plasticity in the T helper 17 lineage. Immunity. 2009; 30:92–107. [PubMed: 19119024]
17. Yao Z, Kanno Y, Kerenyi M, Stephens G, Durant L, Watford WT, Laurence A, Robinson GW, Shevach EM, Moriggl R, Hennighausen L, Wu C, O'Shea JJ. Nonredundant roles for Stat5a/b in directly regulating Foxp3. Blood. 2007; 109:4368–4375. [PubMed: 17227828]
18. Durant L, Watford WT, Ramos HL, Laurence A, Vahedi G, Wei L, Takahashi H, Sun HW, Kanno Y, Powrie F, O'Shea JJ. Diverse targets of the transcription factor STAT3 contribute to T cell pathogenicity and homeostasis. Immunity. 2010; 32:605–615. [PubMed: 20493732]
19. Di Maira G, Salvi M, Arrigoni G, Marin O, Sarno S, Brustolon F, Pinna LA, Ruzzene M. Protein kinase CK2 phosphorylates and upregulates Akt/PKB. Cell Death Differ. 2005; 12:668–677. [PubMed: 15818404]
20. Torres J, Pulido R. The tumor suppressor PTEN is phosphorylated by the protein kinase CK2 at its C terminus. Implications for PTEN stability to proteasome-mediated degradation. J Biol Chem. 2001; 276:993–998. [PubMed: 11035045]
21. Zheng Y, Qin H, Stuart F, Deng L, Litchfield DW, Terfferi A, Pardanani A, Lin FT, Li J, Sha B, Benveniste EN. A CK2-dependent mechanism for activation of the JAK-STAT signaling pathway. Blood. 2011; 118:156–166. [PubMed: 21527517]
22. Fontenot JD, Rasmussen JP, Williams LM, Dooley JL, Farr AG, Rudensky AY. Regulatory T cell lineage specification by the forkhead transcription factor foxp3. Immunity. 2005; 22:329–341. [PubMed: 15780990]
23. Qin H, Wang L, Feng T, Elson CO, Niyongere SA, Lee SJ, Reynolds SL, Weaver CT, Roarty K, Serra R, Benveniste EN, Cong Y. TGF-β promotes Th_{17} cell development through inhibition of SOCS3. J Immunol. 2009; 183:97–105. [PubMed: 19535626]
24. Zou C, Wang Y, Shen Z. 2-NBDG as a fluorescent indicator for direct glucose uptake measurement. J Biochem Biophys Methods. 2005; 64:207–215. [PubMed: 16182371]
25. Qin H, Yeh WI, De Sarno P, Holdbrooks AT, Liu Y, Muldowney MT, Reynolds SL, Yanagisawa LL, Fox THI, Park K, Harrington LE, Raman C, Benveniste EN. Signal transducer and activator of transcription-3/suppressor of cytokine signaling-3 (STAT3/SOCS3) axis in myeloid cells regulates neuroinflammation. Proc Natl Acad Sci U S A. 2012; 109:5004–5009. [PubMed: 22411837]
26. Wang Y, Godec J, Ben-Aissa K, Cui K, Zhao K, Pucsek AB, Lee YK, Weaver CT, Yagi R, Lazarevic V. The transcription factors T-bet and Runx are required for the ontogeny of pathogenic interferon-gamma-producing T helper 17 cells. Immunity. 2014; 40:355–366. [PubMed: 24530058]
27. Jager A, Dardalhon V, Sobel RA, Bettelli E, Kuchroo VK. Th1, Th17, and Th9 effector cells induce experimental autoimmune encephalomyelitis with different pathological phenotypes. J Immunol. 2009; 183:7169–7177. [PubMed: 19890056]
28. Bettelli E, Pagany M, Weiner HL, Linington C, Sobel RA, Kuchroo VK. Myelin oligodendrocyte glycoprotein-specific T cell receptor transgenic mice develop spontaneous autoimmune optic neuritis. J Exp Med. 2003; 197:1073–1081. [PubMed: 12732654]
29. Liu Y, Holdbrooks AT, De Sarno P, Rowse AL, Yanagisawa LL, McFarland BC, Harrington LE, Raman C, Sabbaj S, Benveniste EN, Qin H. Therapeutic efficacy of suppressing the JAK/STAT pathway in multiple models of experimental autoimmune encephalomyelitis. J Immunol. 2014; 192:59–72. [PubMed: 24323580]
30. Sarbassov DD, Ali SM, Sengupta S, Sheen JH, Hsu PP, Bagley AF, Markhard AL, Sabatini DM. Prolonged rapamycin treatment inhibits mTORC2 assembly and Akt/PKB. Mol Cell. 2006; 22:159–168. [PubMed: 16603397]
31. Zheng Y, Collins SL, Lutz MA, Allen AN, Kole TP, Zarek PE, Powell JD. A role for mammalian target of rapamycin in regulating T cell activation versus anergy. J Immunol. 2007; 178:2163–2170. [PubMed: 17277121]
32. Miskov-Zivanov N, Turner MS, Kane LP, Morel PA, Faeder JR. The duration of T cell stimulation is a critical determinant of cell fate and plasticity. Sci Signal. 2013; 6:ra97. [PubMed: 24194584]

Author Manuscript Author Manuscript Author Manuscript Author Manuscript

33. Turner MS, Kane LP, Morel PA. Dominant role of antigen dose in CD4+Foxp3+ regulatory T cell induction and expansion. J Immunol. 2009; 183:4895–4903. [PubMed: 19801514]
34. McGuire DJ, Rowse AL, Li H, Peng BJ, Sestero CM, Cashman KS, De Sarno P, Raman C. CD5 enhances Th17-cell differentiation by regulating IFN-gamma response and RORgammat localization. Eur J Immunol. 2014; 44:1137–1142. [PubMed: 24356888]
35. Sestero CM, McGuire DJ, De Sarno P, Brantley EC, Soldevila G, Axtell RC, Raman C. CD5-Dependent CK2 Activation Pathway Regulates Threshold for T Cell Anergy. J Immunol. 2012; 189:2918–2930. [PubMed: 22904299]
36. Weaver CT, Harrington LE, Mangan PR, Gavrieli M, Murphy KM. Th17: an effector CD4 T cell lineage with regulatory T cell ties. Immunity. 2006; 24:677–688. [PubMed: 16782025]
37. Mangan PR, Harrington LE, O'Quinn DB, Helms WS, Bullard DC, Elson CO, Hatton RD, Wahl SM, Schoeb TR, Weaver CT. Transforming growth factor-β induces development of the TH17 lineage. Nature. 2006; 441:231–234. [PubMed: 16648837]
38. Kim H, Choi K, Kang H, Lee SY, Chi SW, Lee MS, Song J, Im D, Choi Y, Cho S. Identification of a Novel Function of CX-4945 as a Splicing Regulator. PLoS One. 2014; 9:e94978. [PubMed: 24743259]
39. Lou DY, Dominguez I, Toselli P, Landesman-Bollag E, O'Brien C, Seldin DC. The alpha catalytic subunit of protein kinase CK2 is required for mouse embryonic development. Mol Cell Biol. 2008; 28:131–139. [PubMed: 17954558]
40. Lee Y, Awasthi A, Yosef N, Quintana FJ, Xiao S, Peters A, Wu C, Kleinewietfeld M, Kunder S, Hafler DA, Sobel RA, Regev A, Kuchroo VK. Induction and molecular signature of pathogenic T(H)17 cells. Nat Immunol. 2012; 13:991–999. [PubMed: 22961052]
41. Michalek RD V, Gerriets A, Jacobs SR, Macintyre AN, MacIver NJ, Mason EF, Sullivan SA, Nichols AG, Rathmell JC. Cutting edge: distinct glycolytic and lipid oxidative metabolic programs are essential for effector and regulatory CD4+ T cell subsets. J Immunol. 2011; 186:3299–3303. [PubMed: 21317389]
42. MacIver NJ, Michalek RD, Rathmell JC. Metabolic regulation of T lymphocytes. Annu Rev Immunol. 2013; 31:259–283. [PubMed: 23298210]
43. Dang EV, Barbi J, Yang HY, Jinasena D, Yu H, Zheng Y, Bordman Z, Fu J, Kim Y, Yen HR, Luo W, Zeller K, Shimoda L, Topalian SL, Semenza GL, Dang CV, Pardoll DM, Pan F. Control of T(H)17/T(reg) balance by hypoxia-inducible factor 1. Cell. 2011; 146:772–784. [PubMed: 21871655]
44. Gerriets VA, Kishton RJ, Nichols AG, Macintyre AN, Inoue M, Ilkayeva O, Winter PS, Liu X, Priyadharshini B, Slawinska ME, Haeberli L, Huck C, Turka LA, Wood KC, Hale LP, Smith PA, Schneider MA, MacIver NJ, Locasale JW, Newgard CB, Shinohara ML, Rathmell JC. Metabolic programming and PDHK1 control CD4+ T cell subsets and inflammation. J Clin Invest. 2015; 125:194–207. [PubMed: 25437876]
45. Codarri L, Gyulveszi G, Tosevski V, Hesske L, Fontana A, Magnenat L, Suter T, Becher B. RORgammat drives production of the cytokine GM-CSF in helper T cells, which is essential for the effector phase of autoimmune neuroinflammation. Nat Immunol. 2011; 12:560–567. [PubMed: 21516112]
46. El-Behi M, Ciric B, Dai H, Yan Y, Cullimore M, Safavi F, Zhang GX, Dittel BN, Rostami A. The encephalitogenicity of T(H)17 cells is dependent on IL-1- and IL-23-induced production of the cytokine GM-CSF. Nat Immunol. 2011; 12:568–575. [PubMed: 21516111]
47. Ulges A, Witsch EJ, Pramanik G, Klein M, Birkner K, Buhler U, Wasser B, Luessi F, Stergiou N, Dietzen S, Bruhl TJ, Bohn T, Bundgen G, Kunz H, Waisman A, Schild H, Schmitt E, Zipp F, Bopp T. Protein kinase CK2 governs the molecular decision between encephalitogenic TH17 cell and Treg cell development. Proc Natl Acad Sci U S A. 2016; 113:10145–10150. [PubMed: 27555590]
48. Ulges A, Klein M, Reuter S, Gerlitzki B, Hoffmann M, Grebe N, Staudt V, Stergiou N, Bohn T, Bruhl TJ, Muth S, Yurugi H, Rajalingam K, Bellinghausen I, Tuettenberg A, Hahn S, Reissig S, Haben I, Zipp F, Waisman A, Probst HC, Beilhack A, Buchou T, Filhol-Cochet O, Boldyreff B, Breloer M, Jonuleit H, Schild H, Schmitt E, Bopp T. Protein kinase CK2 enables regulatory T cells to suppress excessive TH2 responses in vivo. Nat Immunol. 2015; 12:568–575.

Author Manuscript Author Manuscript Author Manuscript Author Manuscript

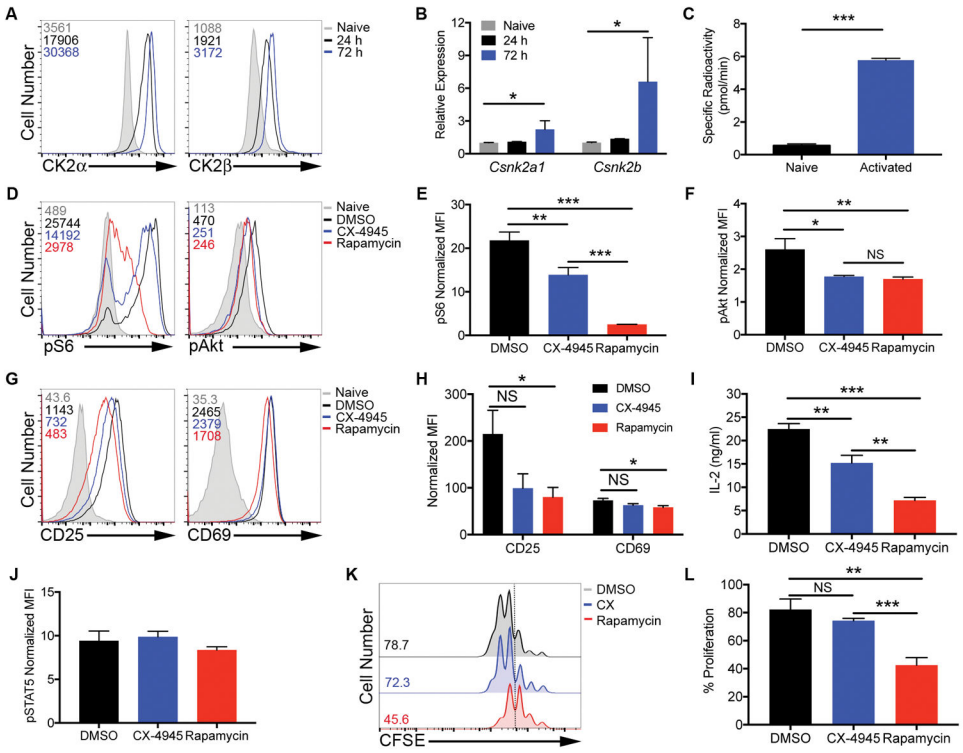

Figure 1. CK2 Kinase Activity is Induced Upon CD4$^+$ T Cell Activation and Promote Akt/mTOR Signaling, but is Not Required for Activation or Proliferation

(A, B) CD4$^+$ T cells were activated with plate-bound anti-CD3 (10 μg/ml) and soluble anti-CD28 (1 μg/ml) antibodies. **(A)** At 24 and 72 h, cells were stained for intracellular CK2α and CK2β; numbers represent corresponding mean fluorescence intensities (MFIs), and data are representative of 3 independent experiments. **(B)** RNA was extracted and qPCR performed using primers for *Csnk2a1* and *Csnk2b* (n=3). **(C)** At 72 h, naïve and activated cells were assayed for CK2 kinase activity. Data represent mean of 2 technical replicates, and are representative of 3 independent experiments. **(D–J)** Naïve CD4$^+$ T cells were activated in the absence or presence of CX-4945 (2 μM) or rapamycin (100 nM) for 24 h. **(D–F)** Cells were stained for phosphorylated S235/236 S6 kinase and phosphorylated S473 Akt. **(D)** Representative histograms and **(E, F)** MFIs normalized to the corresponding naïve control +/− SEM are shown (n=3). **(G–I)** Cells were stained for surface expression of the activation markers CD25 and CD69. **(G)** Representative histograms and **(H)** MFIs normalized to the corresponding naïve control +/− SEM are shown (n=3). **(I)** IL-2 was detected in the supernatant by ELISA. Concentrations +/− SEM are shown (n=3). **(J)** Cells were stained for phosphorylated Y694 STAT5. MFIs normalized to the corresponding naïve control +/− SEM are shown (n=3). **(K, L)** Naïve CD4$^+$ T cells were incubated with CFSE dye and activated with anti-CD3 and anti-CD28 antibodies in the absence or presence of CX-4945 or rapamycin for 72 h, and proliferation assessed by CFSE dilution. **(K)** Representative histograms and **(L)** frequencies of cells undergoing 3 or more divisions +/− SEM (n=3). *p<0.05, **p<0.01, ***p<0.001.

Author Manuscript
Author Manuscript
Author Manuscript
Author Manuscript

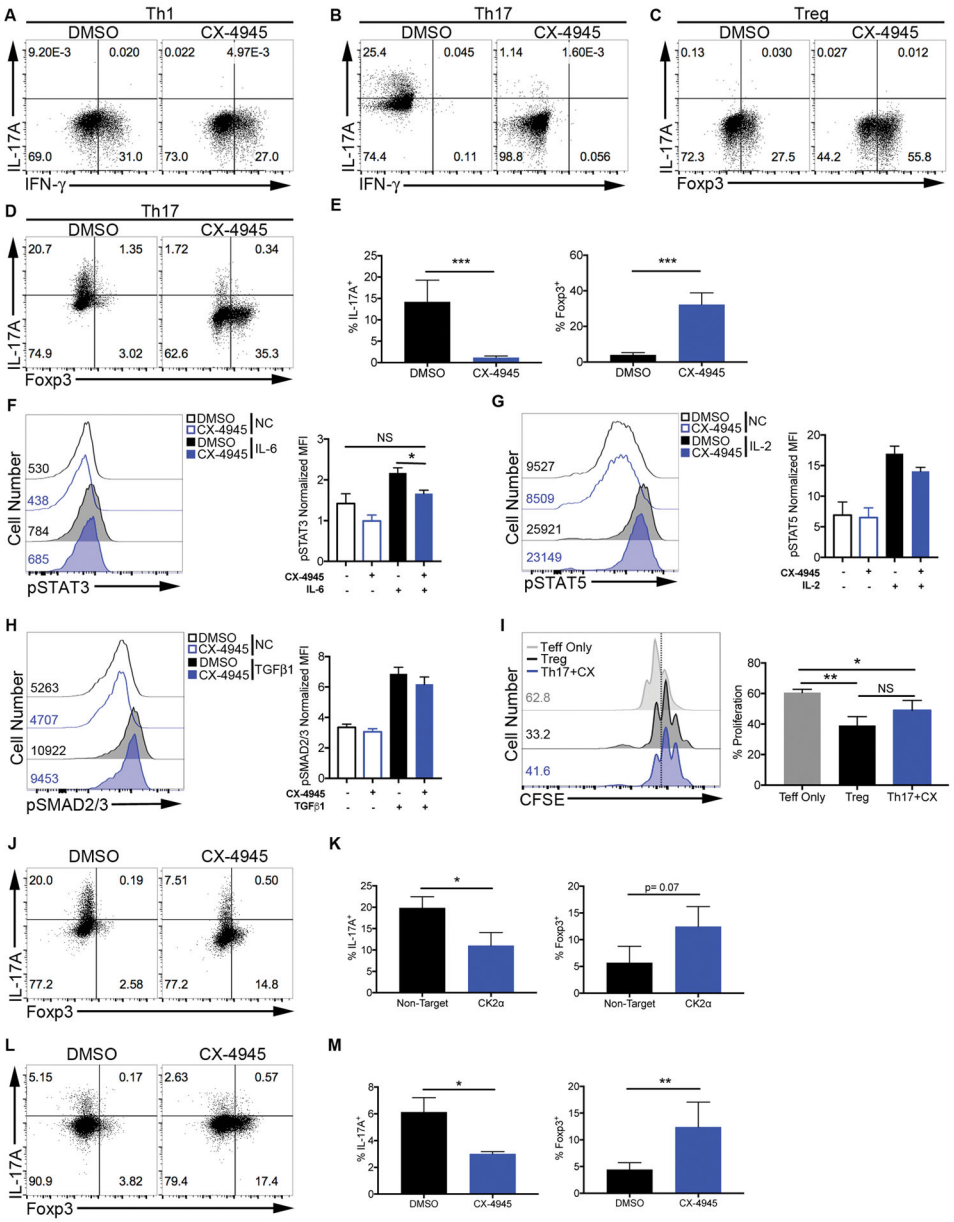

Figure 2. Inhibition of CK2 Selectively Suppresses Th17 Cell Differentiation and Promotes Tregs

(A, B) T cells were cultured in **(A)** Th1 and **(B)** Th17 conditions in the absence or presence of CX-4945 (2 μM) and at 72 h stained for IFN-γ and IL-17A. **(C, D)** Cells were cultured in **(C)** Treg and **(D)** Th17 conditions in the absence or presence of CX-4945 and at 72 h stained for Foxp3 and IL-17A. Data are representative of at least 3 independent experiments. **(E)** Mean frequencies of IL-17A$^+$ and Foxp3$^+$ cells in Th17 conditions +/− SEM are shown (n=6). **(F–I)** T cells were activated for 24 h, cultured in serum free media +/− CX-4945 (2 μM) for 4 h, then stimulated with **(F)** IL-6 (10 ng/ml) for 2 h, **(G)** IL-2 (5 ng/ml) for 30 min, or **(H)** TGFβ1 (5 ng/ml) for 30 min, and stained for phosphorylated Y705 STAT3, Y694 STAT5 or S463/465 Smad2 and S465/467 Smad3, respectively. NC: no cytokine. Representative histograms and MFIs normalized to isotype controls +/− SEM are shown

Author Manuscript Author Manuscript Author Manuscript Author Manuscript

(n=3). **(I)** *Il17f*$^{Thy1.1}$.*Foxp3*^{GFP} T cells were polarized to the Th17 phenotype in the presence of CX-4945 (Th17+CX) or the Treg phenotype. GFP^{+} cells were sorted and co-cultured with CFSE-labeled effector T cells and proliferation assessed by CFSE dilution after 72 h. Representative histograms and mean frequencies of cells undergoing 3 or more divisions +/− SEM are shown (n=3). **(J, K)** T cells were transfected with the indicated siRNAs and polarized in Th17 conditions for 72 h. **(J)** A representative FACS plot and **(K)** mean frequencies of IL-17A^{+} and Foxp3^{+} cells +/− SEM are shown (n=3). **(L, M)** PBMCs were isolated from human blood and cultured in Th17 conditions for 6 days. **(L)** A representative FACS plot and **(M)** mean frequencies of IL-17A^{+} and Foxp3^{+} cells +/− SEM are shown (n=3). *p<0.05, **p<0.01, ***p<0.001.

Author Manuscript Author Manuscript Author Manuscript Author Manuscript

A

# Genes Differentially Expressed	1538
# Genes Upregulated by CX-4945	650
# Genes Downregulated by CX-4945	888

B

Pathway	% Overlap	FDR-q
HALLMARK_HYPOXIA	13.500	1.4E-35
GSE39820_CTRL_VS_IL1B_IL6_IL23A_CD4_TCELL_DN	13.000	4.6E-32
GSE39820_CTRL_VS_TGFBETA3_IL6_CD4_TCELL_DN	10.500	1.7E-23
GSE39820_CTRL_VS_IL1B_IL6_CD4_TCELL_DN	8.500	2.3E-17
GSE39820_CTRL_VS_TGFBETA1_IL6_CD4_TCELL_DN	8.000	5.2E-16
HALLMARK_GLYCOLYSIS	3.500	1.2E-05
HALLMARK_IL6_JAK_STAT3_SIGNALING	3.448	0.00632
HALLMARK_MTORC1_SIGNALING	3.000	0.00011

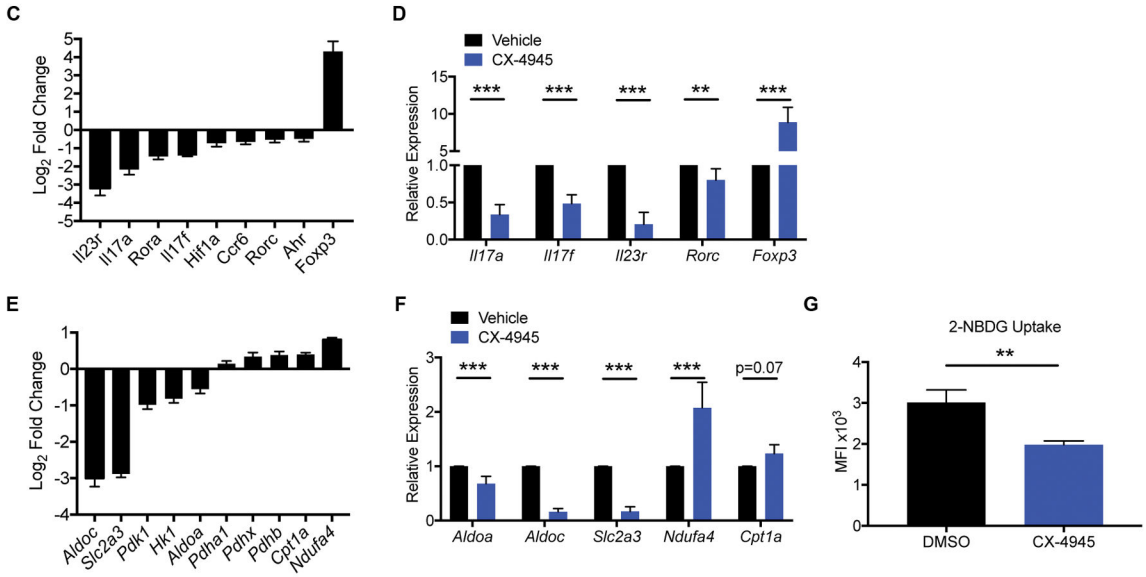

Figure 3. Inhibition of CK2 Kinase Activity Suppresses Th17- and Pathogenic Th17-associated Effector and Metabolic Gene Expression

Naïve $CD4^+$ T cells were cultured in Th17 conditions in the absence or presence of CX-4945 (2 μM). At 72 h, RNA was extracted from cells from 3 independent experiments, and RNA-seq performed. **(A)** Summary of genes differentially regulated by CX-4945 treatment using the following cutoffs are shown: $p<0.05$, fold change >2 or <−2. **(B)** Gene Set Enrichment Analysis (Broad Institute) was performed on 134 genes selected on the following parameters: RPKM>20, fold-change <−2 and $p<0.05$. The percent overlap and FDR-q value of representative gene sets relevant to Th17 cell biology are shown. **(C)** The $\log_2$ fold change from vehicle control of genes associated with the Th17 effector program and Foxp3 are shown (n=3). **(D)** A panel of Th17 effector genes was validated by qPCR (n=6). **(E)** The $\log_2$ fold change from vehicle control of genes associated with glycolysis and oxidative phosphorylation are shown (n=3). **(F)** A panel of genes involved in metabolic pathways was validated by qPCR. (n=6). **(G)** Naïve $CD4^+$ T cells were cultured in Th17 cell conditions in the absence or presence of CX-4945 for 72 h and glycolytic activity measured by 2-NBDG uptake. MFIs +/− SEM are shown (n=3). **p<0.01, ***p<0.001.

Author Manuscript Author Manuscript Author Manuscript Author Manuscript

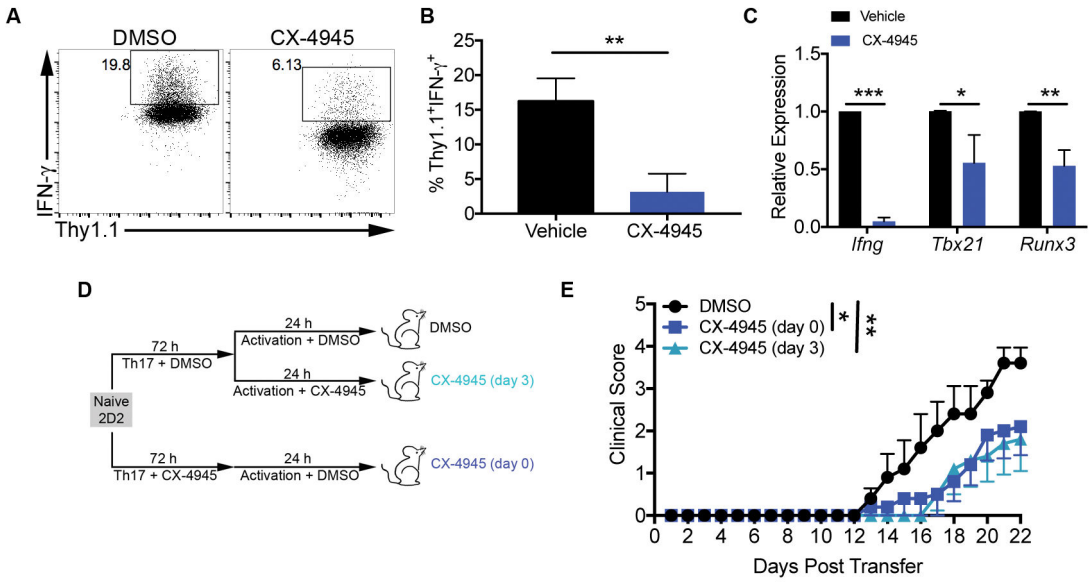

Figure 4. CX-4945 Treatment Suppresses the Pathogenicity of Th17 Cells

(A–C) Naïve CD4$^+$ T cells from *Il17f*$^{Thy1.1}$.*Foxp3*^{GFP} reporter mice were cultured in Th17 conditions. At 72 h Thy1.1$^+$GFP$^-$ cells were sorted and reactivated with anti-CD3 and anti-CD28 antibodies and IL-12 (10 ng/ml) in the absence or presence of CX-4945 (2 μM). **(A, B)** After 48 h of restimulation, cells were stained for IFN-γ. **(A)** Representative FACS plots and **(B)** mean frequencies of Thy1.1$^+$IFN-γ$^+$ cells +/− SEM are shown (n=3). **(C)** At 72 h, mRNA was extracted and gene expression analyzed by qRT-PCR. Data represent the mean relative expression to DMSO control (n=3). **(D)** 2D2 T cells were activated and polarized under Th17 conditions in the absence or presence of CX-4945 (2 μM) [CX-4945 (day 0)]. On day 3, cells were reactivated for 24 h. Cells that were polarized in the absence of CX-4945 were reactivated in the absence (DMSO) or presence of CX-4945 [CX-4945 (day 3)]. On day 4, 2 x 10^6 cells from each condition were transferred into *Rag1*$^{-/-}$ recipient mice. **(E)** Mice were scored daily for symptoms of classical EAE. Data are pooled form 2 separate experiments; n=5/group. *p<0.05, **p<0.01, ***p<0.001.

Author Manuscript Author Manuscript Author Manuscript Author Manuscript

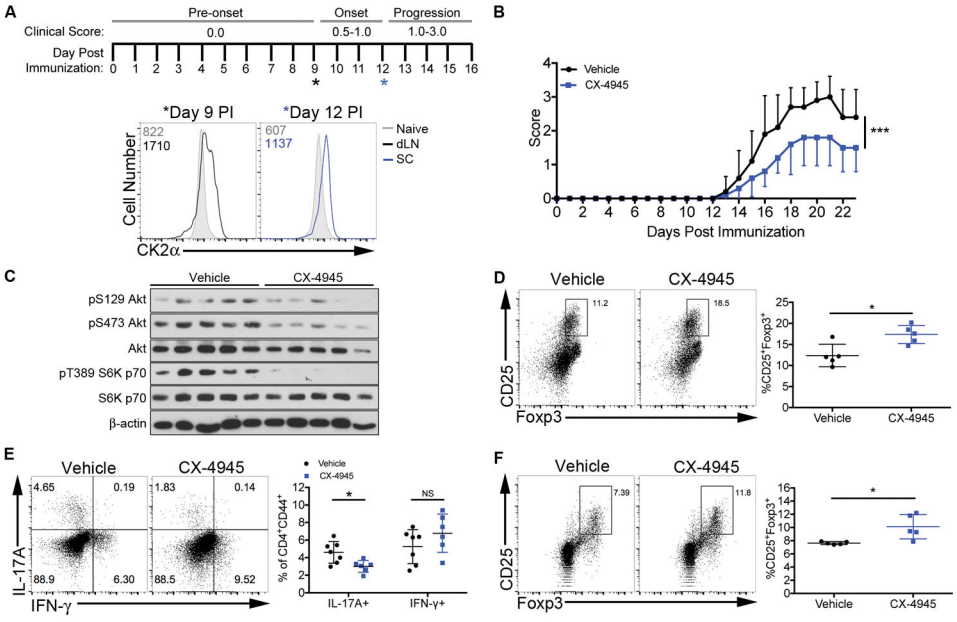

Figure 5. ***In Vivo*** **CX-4945 Pre-treatment Suppresses Th17 Cell Differentiation and Promotes Tregs During EAE**

(A) A schematic of disease induction, scoring and progression is shown with asterisks indicating time-points for CK2α detection. At days 9 and 12 post immunization (PI), cells were enriched from the draining lymph nodes (dLN) and spinal cord, respectively, and stained for intracellular CK2α. Data are representative of at least 3 independent experiments. **(B–D)** Mice were treated with CX-4945 (20 mg/kg/day) or sodium phosphate buffer (Vehicle) from 7 days before immunization throughout disease. Data are from 1 representative experiment of at least 2 independent experiments. **(B)** Clinical scores from days 0 to 23 PI are show; n=5/group. **(C)** On day 9, $CD4^+$ T cells were enriched from the spleens via magnetic selection, lysed and immunoblotted for phosphorylated S129 and S473 Akt and T389 and S371 S6K p70; n=5/group. **(D)** On day 23, mononuclear cells were enriched from the spinal cord and Tregs identified by CD25 and Foxp3 staining; n=5/group. **(E, F)** Mice were treated with vehicle or CX-4945 (20 mg/kg/day) via oral gavage from days 0 to 7 PI. Data were pooled from 2 independent experiments. **(E)** At day 7, $CD4^+$ T cells from the dLNs were stained for IL-17A and IFN-γ; n=8/group. **(F)** At day 7, $CD4^+$ T cells from the spleens were stained for CD25 and Foxp3; n=5/group. *p<0.05, ***p<0.001.

Author Manuscript Author Manuscript Author Manuscript Author Manuscript

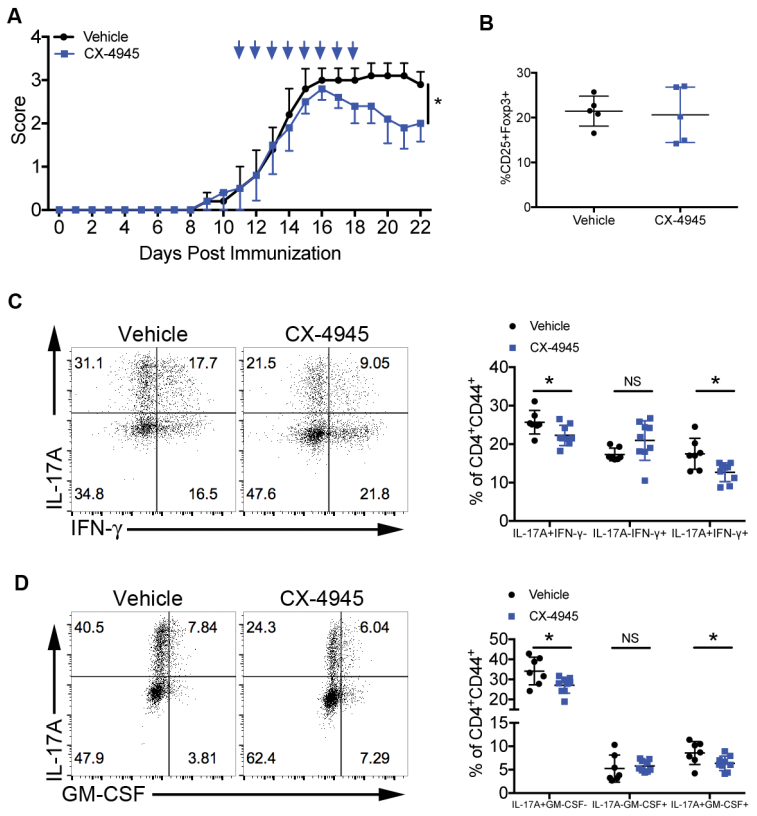

Figure 6. CX-4945 Therapeutic Treatment Suppresses Th17 Cell Differentiation and Reduces Disease Severity During EAE

(A, B) Mice were treated with vehicle or CX-4945 via oral gavage for 8 days beginning at the onset of clinical symptoms. Data are from 1 representative experiment of at least 2 independent experiments. **(A)** Clinical scores from day 0 to 22 PI are shown; n=5/group. **(B)** At day 22, during disease resolution, mononuclear cells were enriched from the spinal cord and Tregs identified by CD25 and Foxp3 staining; n=5/group. **(C, D)** Mice were treated with vehicle or CX-4945 beginning on day 7 PI. At disease peak, effector T cells from the spinal cords were stained for **(C)** IL-17A and IFN-γ or **(D)** IL-17A and GM-CSF. Representative flow plots and frequencies of single and double positive cells +/− SEM are shown. Data were pooled from 3 independent experiments; vehicle, n=6; CX-4945, n=8. *p<0.05.